

Multiplicity distributions and long range rapidity correlations

T. Lappi^{a,b}

^a*Department of Physics, P.O. Box 35, 40014 University of Jyväskylä, Finland*

^b*Helsinki Institute of Physics, P.O. Box 64, 00014 University of Helsinki, Finland*

Abstract

The physics of the initial conditions of heavy ion collisions is dominated by the nonlinear gluonic interactions of QCD. These lead to the concepts of parton saturation and the Color Glass Condensate (CGC). We discuss recent progress in calculating multi-gluon correlations in this framework, prompted by the observation that these correlations are in fact easier to compute in a dense system (nucleus-nucleus) than a dilute one (proton-proton).

Keywords:

1. Introduction

Bulk particle production in relativistic collisions around midrapidity originates from small x degrees of freedom, predominantly gluons, in the wavefunctions of the colliding hadrons or nuclei. At large energies these gluons form a dense system characterized by a *saturation scale* Q_s . The degrees of freedom with $p_T \lesssim Q_s$ are fully nonlinear Yang-Mills fields with large field strength $A_\mu \sim 1/g$ and occupation numbers $\sim 1/\alpha_s$; they can therefore be understood as classical fields radiated from the large x partons. Because of their large longitudinal momentum, the large x degrees of freedom are effectively “frozen” during the interaction. They can be described as random color charges drawn from a classical probability distribution $W_y[\rho]$ that depends on the rapidity cutoff $y = \ln 1/x$ separating the large and small x degrees of freedom. The dependence of $W_y[\rho]$ on y is described by a Wilsonian renormalization group equation known by the acronym JIMWLK. Note that while this description is inherently nonperturbative, it is still based on a weak coupling argument, because the classical approximation requires $\alpha_s(Q_s)$ to be small and therefore $Q_s \gg \Lambda_{\text{QCD}}$. The Color Glass Condensate (CGC, for reviews see [1]) is a systematic effective theory (effective because the large x part of the wavefunction is integrated out) description of the classical small x degrees of freedom.

The term glasma [2] refers to the coherent, classical field configuration resulting from the collision of two such objects CGC. The glasma fields are initially longitudinal, whence the “glasma flux tube” [3, 4] picture. More importantly for computing multigluon correlations, they are boost invariant (to leading order in the QCD coupling) and depend on the transverse coordinate with a characteristic correlation length $1/Q_s$. There are several signals in the RHIC data [5, 6] that point to strong correlations originating from the initial stage of the collision. The glasma fields provide a natural framework for understanding these effects, although much work is still left to do in understanding the interplay with purely geometrical effects from the fluctuating positions of the nucleons in the colliding nuclei [7, 8].

We shall first describe some general observations on computing multigluon correlations in the glasma, arguing in Sec. 2 that they are in some sense simpler to compute in a collision of two

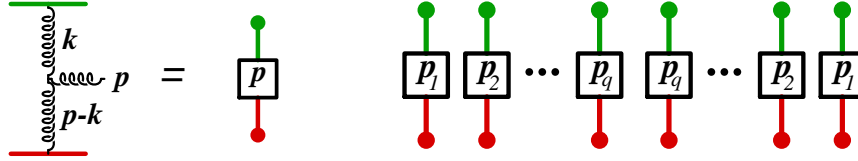


Figure 1: Left: Building block, Lipatov vertex coupled to two sources. Right: combinatorics of the sources. The combinatorial problem is to connect the dots on the upper and lower side (left- and right moving sources) pairwise.

dense, saturated nuclear wavefunctions than in the dilute limit (see Ref. [9] for a more formal discussion). We shall then, in Sec. 3 discuss one application of these ideas to computing the multiplicity distribution of gluons in the collision before moving to the leading $\ln 1/x$ rapidity dependence of the correlation in Sec. 4.

2. Multigluon correlations in the glasma

The gluon fields in the glasma are nonperturbatively strong, $A_\mu \sim 1/g$. This means that the gluon multiplicity is $N \sim 1/\alpha_s$. For a fixed configuration of the classical color sources it is well known that the multiplicity distribution of produced gluons is Poissonian, i.e. $\langle N^2 \rangle - \langle N \rangle^2 = \langle N \rangle$. In this case the correlations and fluctuations in the gluon multiplicity are all quantum effects that appear only starting from the one-loop level, i.e. suppressed by a power of the coupling constant α_s . The computation in the CGC framework does not end here, however. To calculate the moments of the gluon multiplicity distribution one must first calculate the gluon spectra for fixed configuration of the color charges ρ and then average over the probability distribution $W_y[\rho(\mathbf{x}_\perp)]$. For the n th moment of the multiplicity distribution, i.e. an n -gluon correlation, the leading order result is

$$\left\langle \frac{dN}{d^3\mathbf{p}_1} \cdots \frac{dN}{d^3\mathbf{p}_n} \right\rangle = \left[\int_{[\rho]} W[\rho_1(y)] W[\rho_2(y)] \frac{dN}{d^3\mathbf{p}_1} \Big|_{\text{LO}} \cdots \frac{dN}{d^3\mathbf{p}_n} \Big|_{\text{LO}} \right], \quad (1)$$

where the subscript “LO” refers to the single gluon spectrum evaluated from the classical field configuration corresponding to a fixed configuration of color charges. This averaging, even after the subsequent subtraction of the appropriate disconnected contributions, introduces a correlation already at the leading order in α_s , i.e. enhanced by an additional $1/\alpha_s$ compared to the quantum correlations. A natural example is the negative binomial distribution that we shall discuss below, whose variance is $\langle N^2 \rangle - \langle N \rangle^2 = \langle N \rangle^2/k + \langle N \rangle$. One must emphasize here that although these contributions arise as formally classical correlations in the effective theory that is the CGC, they are physically also quantum effects, where the weak coupling is compensated by a large logarithm of the energy that has been resummed into the probability distribution $W_y[\rho(\mathbf{x}_\perp)]$. In this sense the leading correlations are present already in the wavefunctions of the colliding objects.

3. Multiplicity distribution

We can then apply this formalism to the calculation of the probability distribution of the number of gluons in the glasma [10]. We shall assume the “AA” power counting of sources that are parametrically strong in g , but nevertheless work to the lowest nontrivial order in the color

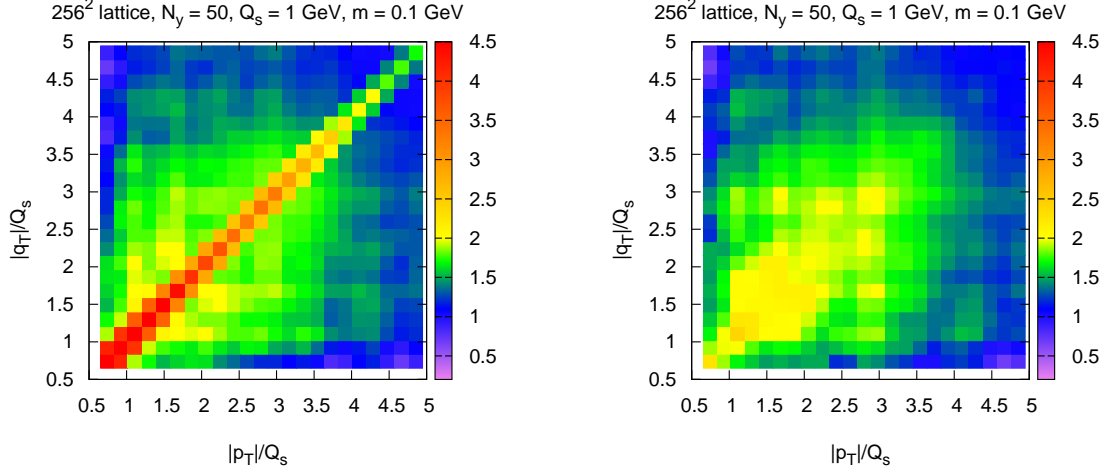


Figure 2: Numerical evaluation of the two-gluon correlation strength in the MV model as a function of the two transverse momenta p_\perp and q_\perp . Left: the correlation strength on the “near side” $|\varphi_p - \varphi_q| < \pi/2$, right: the “away side” $|\varphi_p - \varphi_q| > \pi/2$.

sources. Formally this would correspond to a power counting $\rho \sim g^{\epsilon-1}$ with a small $\epsilon > 0$. In this limit, as we have discussed, the dominant contributions to multiparticle correlations come from diagrams that are disconnected for fixed sources and become connected only after averaging over the color charge configurations. The corresponding two gluon correlation function was computed in Ref. [3] and generalized to a three gluons in Ref. [11]. We shall here sketch the derivation [10] of the general n -gluon correlation in this simplified limit.

Working with the MV model Gaussian probability distribution

$$W[\rho] = \exp \left[- \int d^2 \mathbf{x}_\perp \frac{\rho^a(\mathbf{x}_\perp) \rho^a(\mathbf{x}_\perp)}{g^4 \mu^2} \right] \quad (2)$$

computing the correlations and the multiplicity distribution in the linearized approximation is a simple combinatorial problem. Each gluon is produced from two Lipatov vertices (see fig. 1 left), one in the amplitude and the other in the complex conjugate. The combinatorial factor is obtained by counting the different ways of contracting the sources pairwise (see fig. 1 right). The dominant contributions are the ones that have, in the dilute limit, the strongest infrared divergence which is regulated by the transverse correlation scale of the problem, Q_s . When integrated over the momenta of the produced gluons one obtains the factorial moments of the multiplicity, which define the whole probability distribution. It can be expressed in terms of two parameters, the mean multiplicity \bar{n} , and a parameter k describing the width of the distribution. The result of the combinatorial exercise is that the q th factorial moment m_q (defined as $\langle N^q \rangle$ minus the corresponding disconnected contributions) is

$$m_q = (q-1)! k \left(\frac{\bar{n}}{k} \right)^q \quad \text{with} \quad k \approx \frac{(N_c^2 - 1) Q_s^2 S_\perp}{2\pi} \quad \text{and} \quad \bar{n} = f_N \frac{1}{\alpha_s} Q_s^2 S_\perp. \quad (3)$$

Here S_\perp is the transverse area of the system. These moments define a *negative binomial* distribution with parameters k and \bar{n} , known as a phenomenological observation in high energy hadron and

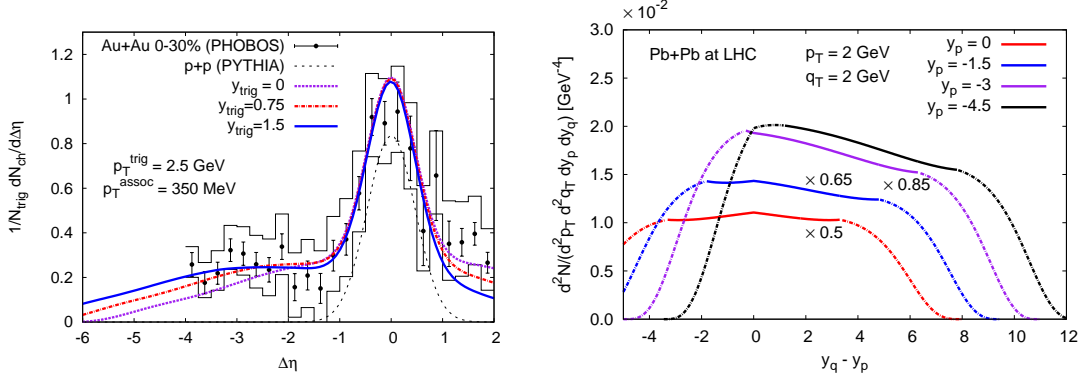


Figure 3: Left: Comparison of a two-particle correlation computed using eq. (5) supplemented with a short-range correlation contribution from PYTHIA with PHOBOS data. Right: Rapidity correlation at LHC energies k_{\perp} -factorization approximation. Plots from [16].

nuclear collisions already for a long time. Also the numerical magnitude of the parameter k obtained from the saturation scale agrees very well with both pp and AA data [12].

This calculation predicts that the k parameter should increase with energy, unlike what is seen in UA5 data. Multiplicity fluctuations in proton-proton collisions at lower energies are still mostly dominated by the dilute edge of the collision system, causing a Poissonian nature (i.e. $k \rightarrow \infty$) of low energy particle emission. Our calculation formally assumes $Q_s^2 S_{\perp} \gg 1$, and we expect the growing behavior of k with energy to eventually take over at high enough energy. Some signs of this are already visible in the LHC $\sqrt{s} = 7$ TeV data [13].

In terms of the glasma flux tube picture this result has a natural interpretation. The transverse area of a typical flux tube is $1/Q_s^2$, and thus there are $Q_s^2 S_{\perp} = N_{\text{FT}}$ independent ones. Each of these radiates particles independently into $N_c^2 - 1$ color states in a Bose-Einstein distribution (see e.g. [14]). A sum of $k \approx N_{\text{FT}}(N_c^2 - 1)$ independent Bose-Einstein-distributions is precisely equivalent to a negative binomial distribution with parameter k . A numerical evaluation [15] of the second moment of the distribution, parametrized in terms of

$$\kappa_2(\mathbf{p}_{\perp}, \mathbf{q}_{\perp}) = Q_s^2 S_{\perp} \left(\frac{d^2 N}{d^2 \mathbf{p}_{\perp} d^2 \mathbf{q}_{\perp}} - \frac{dN}{d^2 \mathbf{p}_{\perp}} \frac{dN}{d^2 \mathbf{q}_{\perp}} \right) / \frac{dN}{d^2 \mathbf{p}_{\perp}} \frac{dN}{d^2 \mathbf{q}_{\perp}} \quad (4)$$

is shown in Fig. 2. It confirms the expectations of [10] that this ratio is of order one and depends only weakly on the momenta $\mathbf{p}_{\perp}, \mathbf{q}_{\perp}$.

4. Rapidity dependence

The general discussion of Sec. 2 on the different nature of multigluon correlations in the “AA” case applies also to the rapidity dependence. Until now we have only been discussing gluon production in a rapidity interval smaller than $1/\alpha_s$. For this we needed only the correlations between the color charges $\rho(\mathbf{x}_{\perp})$ measured at this same rapidity. To understand the rapidity dependence of the correlations one needs also the correlation between color charges at different rapidities, $\langle \rho_y(\mathbf{x}_{\perp}) \rho_{y'}(\mathbf{y}_{\perp}) \rangle$. Also this information is contained in the JIMWLK renormalization group evolution, at least to leading $\ln 1/x$ accuracy [17]. An intuitive description of the resulting correlations is provided by the formulation of JIMWLK as a Langevin equation in the space of Wilson lines

formed from the color charges. In this picture the evolution proceeds in individual trajectories along an increasing rapidity. A first attempt of a realistic estimate of the rapidity dependence of two-gluon correlations is performed in Ref. [16]. Evaluating the two gluon correlation in a dilute limit in a k_\perp -factorized approximation, but keeping the general structure resulting from the JIMWLK evolution leads to the following expression:

$$C(\mathbf{p}, \mathbf{q}) = \frac{\alpha_s^2}{16\pi^{10}} \frac{N_c^2(N_c^2 - 1)S_\perp}{d_A^4 \mathbf{p}_\perp^2 \mathbf{q}_\perp^2} \times \left\{ \int d^2\mathbf{k}_\perp \Phi_{A_1}^2(y_p, \mathbf{k}_\perp) \Phi_{A_2}(y_p, \mathbf{p}_\perp - \mathbf{k}_\perp) \left[\Phi_{A_2}(y_q, \mathbf{q}_\perp + \mathbf{k}_\perp) + \Phi_{A_2}(y_q, \mathbf{q}_\perp - \mathbf{k}_\perp) \right] \right. \\ \left. + \Phi_{A_2}^2(y_q, \mathbf{k}_\perp) \Phi_{A_1}(y_p, \mathbf{p}_\perp - \mathbf{k}_\perp) \left[\Phi_{A_1}(y_q, \mathbf{q}_\perp + \mathbf{k}_\perp) + \Phi_{A_1}(y_q, \mathbf{q}_\perp - \mathbf{k}_\perp) \right] \right\}. \quad (5)$$

Note the very different structure of this correlation compared to one where the gluons would be produced from the same diagram for fixed sources. The two gluon correlation function is proportional to the product of *four* unintegrated gluon distributions, with three of them evaluated at the rapidity of one of the produced gluons and only one at the other. This structure is a direct consequence of the nature of JIMWLK evolution. The resulting correlation is compared to PHOBOS data in fig. 3. The k_\perp -factorized approximation gives a very inaccurate description of the gluon spectrum in the transverse momentum regime $p_\perp \sim Q_s$ where the bulk of the particles are produced [18]. Equation (5) has also been derived in the approximation, true only in the linearized case, that the unequal rapidity correlation of two color charge densities is equal to the unintegrated gluon distribution at the smaller one of these rapidities. As of yet there is no calculation of how much this approximation is violated in the full JIMWLK evolution. The results presented in fig. 3 are therefore not the final word on the subject, although it is reassuring that such a simple approximation seems to agree rather well with the experimental result.

5. Forward-backward multiplicity correlation

Let us conclude by a few remarks on the somewhat puzzling STAR data [6] on backward-forward charged hadron multiplicity correlations, following the discussion in Ref. [8]. The reported forward-backward correlation shows a rapid increase as a function of centrality, and appears to have a strength which cannot be explained by a superposition of pp interactions. The measured quantity is usually reported as a correlation coefficient between the charged hadron multiplicities measured in a forward and a backward rapidity bin (N_F and N_B) within the STAR TPC coverage of two units in pseudorapidity:

$$b = \frac{\langle N_F N_B \rangle - \langle N_F \rangle \langle N_B \rangle}{\langle N_F^2 \rangle - \langle N_F \rangle^2}, \quad (6)$$

where due to the symmetrical placement of the bins around midrapidity the variance $\langle N_F^2 \rangle - \langle N_F \rangle^2$ is the same for both rapidity bins. If the expectation value here were taken over all the events in a centrality bin, correlations would be generated by the different impact parameters (or numbers of wounded nucleons) possible within such a bin¹. This is, however, a too simplified picture of

¹One expects the charged multiplicity to be strongly correlated with impact parameter and if the impact parameter itself can have significant variation within a fixed centrality bin, then spurious correlations whose only origin is the geometry of the collision would be generated.

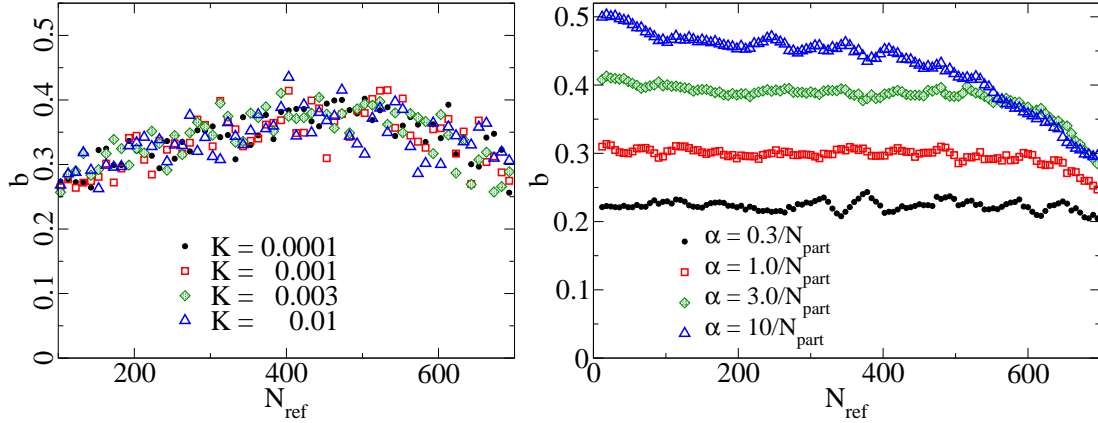


Figure 4: Simple parametrization of a measured forward-backward correlation at fixed reference multiplicity. Left: dependence on strength of the long range correlation K is minimal. Right instead, the observed correlation strength mostly depends on the short range correlation α , i.e. the fluctuations of the multiplicities that are uncorrelated between different rapidities.

what is actually done in the analysis. The nature of the actual quantity reported by STAR is not very explicitly described in the paper; to understand it one must decipher the innocuous-looking statement [6] “... $(N_F, N_B, N_F^2, N_F N_B)$ was obtained on an event-by-event basis as a function of the event multiplicity $[N_R]$...”. In other words the correlation coefficient is not measured averaging over all the events in the bin, but over events with a fixed multiplicity N_R in a third, reference, rapidity window, i.e.

$$b = \frac{\langle N_F N_B \rangle_{N_R} - \langle N_F \rangle_{N_R} \langle N_B \rangle_{N_R}}{\langle N_F^2 \rangle_{N_R} - \langle N_F \rangle_{N_R}^2}. \quad (7)$$

Thus the measured quantity does not describe the relation between *two* but *three* correlated multiplicities. For the largest separations between the forward and backward rapidity windows the reference window is between the two, so there is no reason to assume it to be less correlated with the F, B windows than these are with each other. The analysis in Ref. [8] shows that in the limit of a *maximal* correlation between multiplicities at different rapidities the coefficient “ b ” of eq. (7) reaches a maximum value of $1/2$. The results of a more detailed parametrization including the fluctuations in centrality and two parameters describing the magnitudes of the uncorrelated short range fluctuations $\sim \alpha$ and the long range correlation $\sim K$ are shown in fig. 5. The result remains that while the measured correlation never exceeds $1/2$, its magnitude depends more on the uncorrelated fluctuations than the actual long range correlation. The experimental measurements [6] saturate and, for the most central bins, even exceed this limit derived on very general grounds. Although they do seem to point to very strong correlations, this inconsistency makes their interpretation in terms of any microscopic origin, the glasma or something else, of the correlations difficult.

6. Conclusion

Most experimental observables do not probe the glasma initial state of directly, because the system goes through a complicated time evolution before the hadronization stage. A good candidate

for an experimental probe giving direct access to the initial state is provided by different kinds of correlation measurements. These have indeed been a focus of both experimental and theoretical activity recently. We have argued here that the glasma picture of the initial stages of a heavy ion collision is the natural framework to understand the origin of these correlations.

Acknowledgements. The author is supported by the Academy of Finland, contract 126604.

References

- [1] E. Iancu and R. Venugopalan, The color glass condensate and high energy scattering in QCD, in *Quark gluon plasma*, edited by R. Hwa and X. N. Wang, World Scientific, 2003, arXiv:hep-ph/0303204; H. Weigert, Prog. Part. Nucl. Phys. **55**, 461 (2005), [arXiv:hep-ph/0501087]; F. Gelis, E. Iancu, J. Jalilian-Marian and R. Venugopalan, arXiv:1002.0333 [hep-ph]; T. Lappi, arXiv:1003.1852 [hep-ph].
- [2] T. Lappi and L. McLerran, Nucl. Phys. **A772**, 200 (2006), [arXiv:hep-ph/0602189].
- [3] A. Dumitru, F. Gelis, L. McLerran and R. Venugopalan, Nucl. Phys. **A810**, 91 (2008), [arXiv:0804.3858 [hep-ph]].
- [4] S. Gavin, L. McLerran and G. Moschelli, Phys. Rev. **C79**, 051902 (2009), [arXiv:0806.4718 [nucl-th]].
- [5] J. Putschke, J. Phys. **G34**, S679 (2007), [arXiv:nucl-ex/0701074]; STAR, M. Daugherty, J. Phys. **G35**, 104090 (2008), [arXiv:0806.2121 [nucl-ex]]; PHOBOS, B. Alver *et al.*, J. Phys. **G35**, 104080 (2008), [arXiv:0804.3038 [nucl-ex]].
- [6] STAR, B. I. Abelev *et al.*, Phys. Rev. Lett **103**, 172301 (2009), [arXiv:0905.0237 [nucl-ex]].
- [7] V. P. Konchakovski, M. Hauer, G. Torrieri, M. I. Gorenstein and E. L. Bratkovskaya, Phys. Rev. **C79**, 034910 (2009), [arXiv:0812.3967 [nucl-th]]; A. Bzdak, Phys. Rev. **C80**, 024906 (2009), [arXiv:0902.2639 [hep-ph]]; B. Alver and G. Roland, Phys. Rev. **C81**, 054905 (2010), [arXiv:1003.0194 [nucl-th]]; B. H. Alver, C. Gombeaud, M. Luzum and J.-Y. Ollitrault, arXiv:1007.5469 [nucl-th].
- [8] T. Lappi and L. McLerran, Nucl. Phys. **A832**, 330 (2010), [arXiv:0909.0428 [hep-ph]].
- [9] F. Gelis, T. Lappi and R. Venugopalan, Phys. Rev. **D78**, 054019 (2008), [arXiv:0804.2630 [hep-ph]]; F. Gelis, T. Lappi and R. Venugopalan, Phys. Rev. **D78**, 054020 (2008), [arXiv:0807.1306 [hep-ph]].
- [10] F. Gelis, T. Lappi and L. McLerran, Nucl. Phys. **A828**, 149 (2009), [arXiv:0905.3234 [hep-ph]].
- [11] K. Dusling, D. Fernandez-Fraile and R. Venugopalan, Nucl. Phys. **A828**, 161 (2009), [arXiv:0902.4435 [nucl-th]].
- [12] UA1, G. Arnison *et al.*, Phys. Lett. **B123**, 108 (1983); UA5, G. J. Alner *et al.*, Phys. Lett. **B160**, 193 (1985); UA5, G. J. Alner *et al.*, Phys. Lett. **B160**, 199 (1985); UA5, R. E. Ansorge *et al.*, Z. Phys. **C37**, 191 (1988); PHENIX, S. S. Adler *et al.*, Phys. Rev. **C76**, 034903 (2007), [arXiv:0704.2894 [nucl-ex]]; PHENIX, A. Adare *et al.*, Phys. Rev. **C78**, 044902 (2008), [arXiv:0805.1521 [nucl-ex]].
- [13] ALICE, K. Aamodt *et al.*, Eur. Phys. J. **C68**, 345 (2010), [arXiv:1004.3514 [hep-ex]].
- [14] K. Fukushima, F. Gelis and T. Lappi, Nucl. Phys. **A831**, 184 (2009), [arXiv:0907.4793 [hep-ph]].
- [15] T. Lappi, S. Srednyak and R. Venugopalan, JHEP **01**, 066 (2010), [arXiv:0911.2068 [hep-ph]].
- [16] K. Dusling, F. Gelis, T. Lappi and R. Venugopalan, Nucl. Phys. **A836**, 159 (2010), [arXiv:0911.2720 [hep-ph]].
- [17] F. Gelis, T. Lappi and R. Venugopalan, Phys. Rev. **D79**, 094017 (2008), [arXiv:0810.4829 [hep-ph]]; T. Lappi, Acta Phys. Polon. **B40**, 1997 (2009), [arXiv:0904.1670 [hep-ph]].
- [18] J. P. Blaizot, T. Lappi and Y. Mehtar-Tani, Nucl. Phys. **A846**, 63 (2010), [arXiv:1005.0955 [hep-ph]].